Title

A SYSTEM OF SOILS FOR INCREASING THE VOLUME OF HOMOGENEOUS FIELD BETWEEN THE PARALLEL POLE FACES OF AN ELECTROMAGNET

Author

Nelson, Donald H..

Publication Date

1975-04-14

LBL-3860

A SYSTEM OF COILS FOR INCREASING THE VOLUME OF HOMOGENEOUS FIELD BETWEEN THE PARALLEL POLE FACES OF AN ELECTROMAGNET

Donald H. Nelson
(M. S. thesis)

April 14, 1975

Prepared for the U. S. Energy Research and Development Administration under Contract W-7405-ENG-48

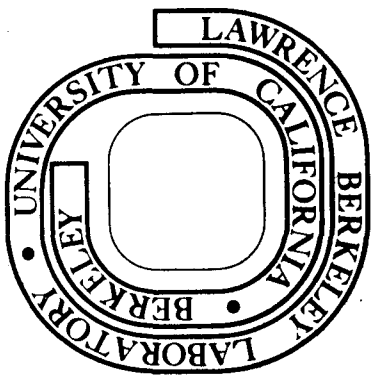

LBL-3860

DISCLAIMER

A System of Coils for Increasing the Volume of Homogeneous Field Between the Parallel Pole Faces of an Electromagnet

By

Donald Henning Nelson

B.S. (University of California) 1962

THESIS

Submitted in partial satisfaction of the requirements for the degree of

MASTER OF SCIENCE

in

Engineering

in the

GRADUATE DIVISION

of the

UNIVERSITY OF CALIFORNIA, BERKELEY

Approved:

J. R. Singer .....

.....

.....

Committee in Charge

.....

Donald H. Nelson

Lawrence Berkeley Laboratory
University of California
Berkeley, California

April 14, 1975

ABSTRACT

The design and evaluation of a system of coils for improving magnetic field homogeneity are discussed. Using only three coil-pairs the duration of NMR spin-echo signals from a sample of H_2O (0.7 cm. diameter x 0.9 cm. long) was increased by an order of magnitude.

ACKNOWLEDGEMENTS

I would like to thank the many people who contributed to the success of this project and in the preparation of this thesis:

Professor J. R. Singer, my research advisor, for suggesting the project, providing inspirational leadership, and guiding the project to a successful conclusion.

L. E. Crooks for always making himself available when I needed assistance, guidance or just a friend to talk to.

Professors J. R. Whinnery and J. R. Woodyard for their careful reading and thoughtful criticism of this thesis.

Dr. S. A. Knight for generously sending to us photographic negatives used for producing printed-circuits.

J. P. Cullen for his advice and assistance on the preparation of printed-circuit-boards. W. L. Zeilinger and his skilled craftsmen for their high-quality workmanship in fabricating the hardware for this project. Paul Salz for cordially contributing his expertise.

Rita McLaughlin for her careful typing of the manuscript.

Finally, I want to dedicate this work to two people:

To Charles Dols, my cherished friend and colleague who encouraged me to enter graduate school, and for three years has advised me on my selection of courses, tutored me when I needed technical assistance and counselled me when my morale needed a boost.

To Jeffrey Nelson, my 11 year old son who always pretended to understand when my school work took priority over other activities.

This work was done partially under the auspices of the U.S. Energy and Research Development Administration.

TABLE OF CONTENTS

Illustrations

INTRODUCTION

Prof. J. R. Singer and his research assistants, L. E. Crooks and J. A. Murphy, are conducting studies on blood circulation,[1,18] water in biological fluids, and leukemia using Nuclear Magnetic Resonance (NMR) Spin-Echo techniques in a Varian Electromagnet. Improvements in discriminating between NMR signals from similar substances require improvements in the homogeneity of the magnetic field.

This thesis is a report of the work we did to improve the homogeneity of the magnet in a region at the center of the magnet aperture.

In July 1973, Prof. J. R. Singer, L. E. Crooks, and D. H. Nelson measured the magnetic field of the 2.50 in. gap x 11.90 in. diameter Varian Magnet located in Room 145 in the Hearst Mining Building at the University of California in Berkeley.[2] After examining the results of those measurements and searching the literature on magnetic field optimization for NMR studies[3,4,5] we decided to increase the volume of homogeneous magnetic field with "electric shims" (i.e. sets of coils installed on the polefaces of the magnet to modify the shape of the magnetic field). In October 1973, in response to letters from Prof. Singer and me, S. A. Knight of the British Petroleum Research Center generously sent to us detailed instructions on the manufacture of "Golay shim Coils" (i.e. poleface coils constructed on printed-circuit boards) and the photographic negatives that he used for producing printed-circuits installed in a 1.0 in. gap x 7.9 in. diameter magnet.

During 1974 (on a part time basis) we designed and fabricated coils, coil holders, and coil current controls. In December 1974, we installed the coils in the magnet and in January 1975,we tested the completed system.

This paper describes the coil system, the magnetic field measurements, and the results achieved.

COORDINATE SYSTEM

Figure 1 shows the coordinate system referred to in this work superimposed on a drawing of the magnet. The coordinate system was constructed to meet the following criteria: 1) B_z, the main component of magnetic induction is positive when the magnet power supply is positive. 2) +y is directed upward (a convention in NMR work). 3) The coordinate system is right handed.

In order to be consistent with common NMR notation, where the y-axis is the spinning axis, it is necessary to depart from the common labeling used in spherical coordinates. Therefore, the y-axis is the polar axis, θ is the polar angle or co-latitude measured from the positive y-axis ($0 \leq \theta \leq \pi$), and ϕ is the azimuthal angle or latitude measured from the positive z-axis ($0 \leq \phi \leq 2\pi$).

Figure 2 is a photograph which shows part of the magnet. The +z axis is parallel to the visible surface of the magnet iron and is directed nominally to the right. The +x axis is directed into the magnet gap toward the left.

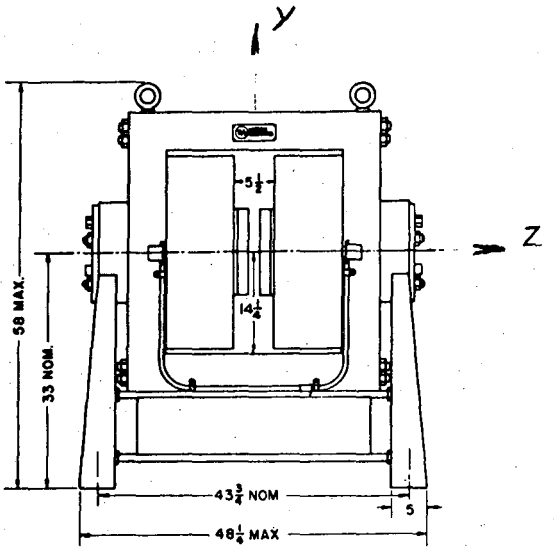

a. Side View

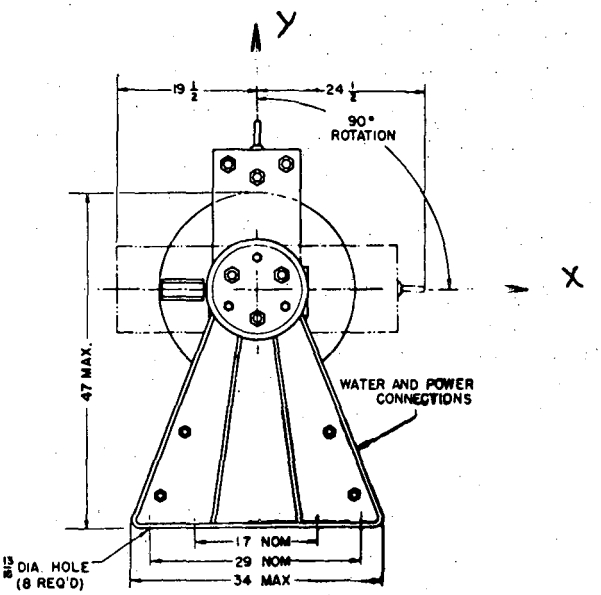

b. End View

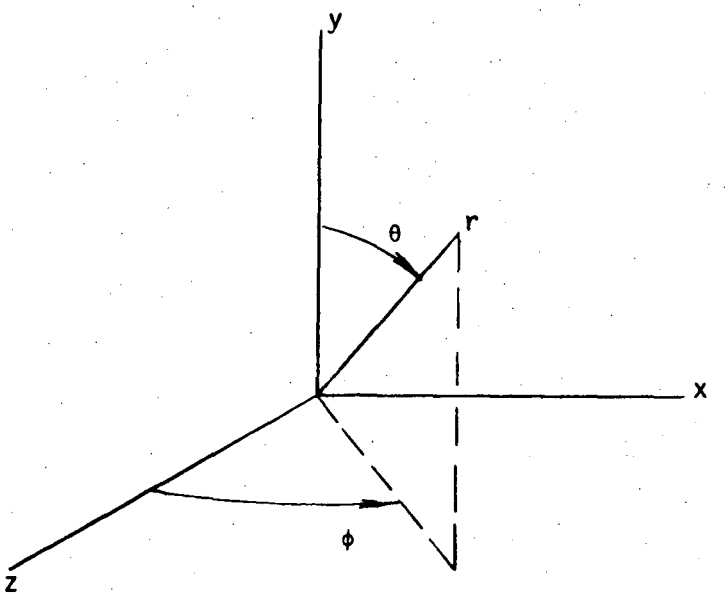

c. Spherical Coordinate System (Unconventional)

XBL 754-1009

Fig. 1 Varian Associates Model V-4012A Twelve Inch Electromagnet and Coordinate System (a & b Courtesy of Varian Associates, Palo Alto, CA.).

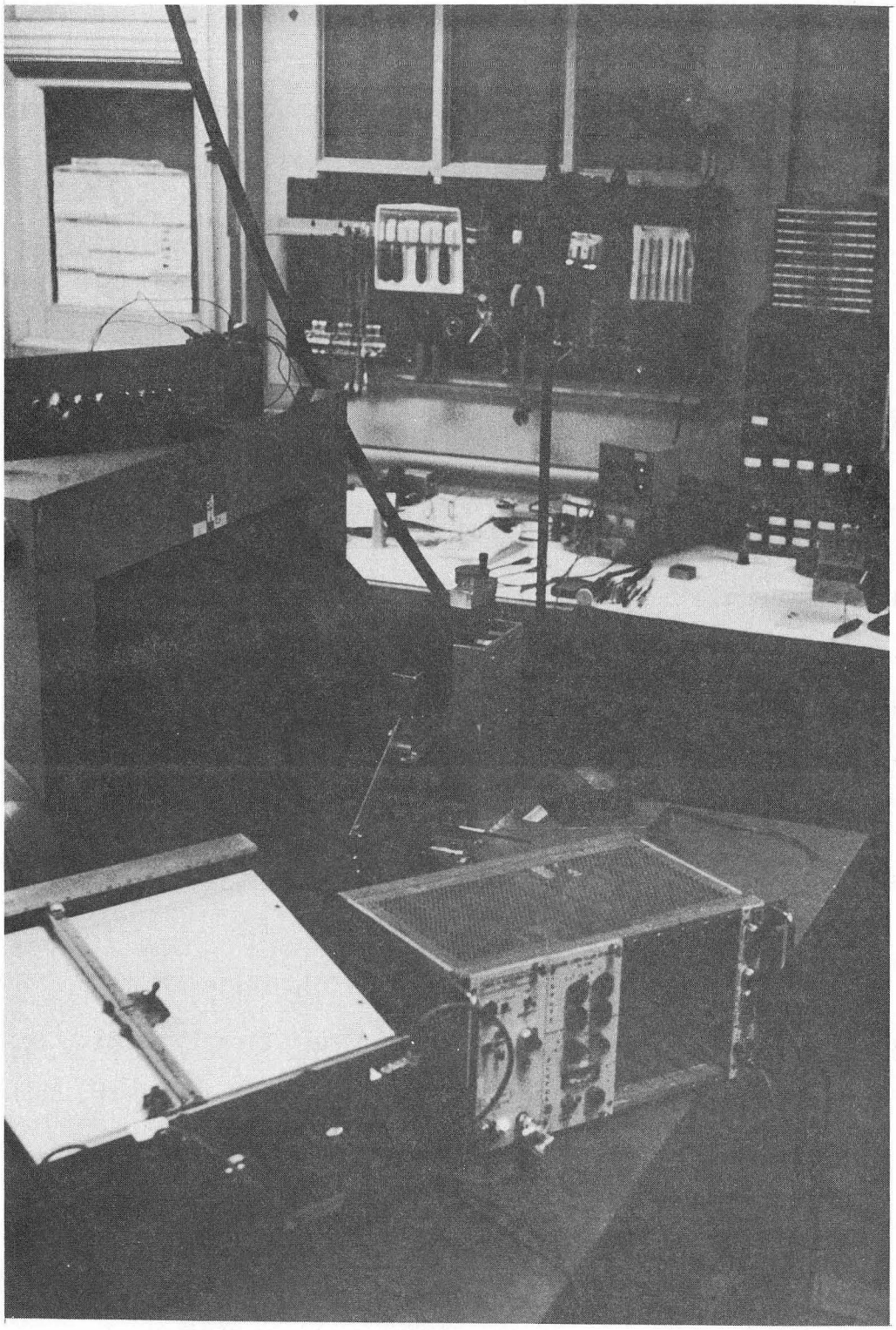

Fig. 2 Varian Magnet Serial No. 529
Room 145 Hearst Mining Bldg., University of California
Berkeley, California

XBB 752-1673

THE THEORY OF ELECTRIC SHIMS

The practice of increasing the volume of homogeneous magnetic field by the judicious placement of current carrying conductors on the pole faces of a magnet is at least 20 years old. In 1955, F. Nelson from Varian Associates filed a patent[3] describing apparatus to achieve this end. And in 1958, M. Golay reported[4] reducing inhomogeneity in a 4mm diameter "Spun-Sample" to less than one part in 10^8 "with a set of 13 homogenizing coils." In 1959, at the Third Annual Workshop on NMR and EPR† Spectroscopy, W. Anderson presented a significant paper on Electric Shims.[5]

The latter paper states that by expanding the magnetic scalar potential, Φ, about the origin of a spherical coordinate system one can determine "the number of independent components in each order of a field derivative." Expanding the magnetic potential about the origin of the coordinate system shown in Fig. 1 leads to Eq. 1.*

$$\Phi(r,\theta,\phi) = \sum_{\ell=0}^{n} \sum_{m=0}^{\ell} r^{\ell} p_{\ell}^{m} (\cos\theta) \left[A_{\ell}^{m} \sin m\phi + B_{\ell}^{m} \cos m\phi \right] \qquad (1)$$

Theoretically, one can construct any field shape by the proper selection of the coefficients $A_{\ell}^{m}, B_{\ell}^{m}$ with n sufficiently large. Because of the orthogonality property of the terms in Eq. 1, the terms represent a minimum set of independent contributions to field shape. Golay shows

*Appendix 1 presents a solution of Laplace's Equation in spherical coordinates based on lecture notes of Prof. J. R. Whinnery.[6]

†NMR and EPR are abbreviations for Nuclear Magnetic Resonance and Electron Paramagnetic Resonance respectively.

that it is possible to produce the terms of the series without requiring "boundary conditons, i.e. coils with currents, in the median plane." His concise statement on the determination of the coil configurations from the potential function is reproduced in full in the next paragraph:

"At the pole faces there will be no discontinuity in the magnetic induction normal to these faces, and the boundary conditions will be satisfied by making the current density within the flat coil on each pole face proportional to and perpendicular to the projection of the magnetic vector on that pole face. Since this projection is the gradient of the potential function in the plane of the pole face, if a sheet of conducting material, such as one copper sheet of photoetching laminate, is cut along the contours of this potential function, and if currents of equal magnitude are caused to circulate in each conducting band between two adjacent contour lines, this will generate the magnetic field deriveable from that particular potential function."

The relationship between Eq. 1 and the order of a field derivative is illustrated by setting n = 1 and examining the resulting terms of Eq. 1. (Use table I, Appendix I for evaluating the Associated-Legendre -Polynomials).

$$\Phi(n = 1) = \sum_{\ell=0}^{1} \sum_{m=0}^{\ell} r^{\ell} p_{\ell}^{m} \ (\cos\theta) \left[A_{\ell}^{m} \sin m\phi + B_{\ell}^{m} \cos m\phi \right] \qquad (2)$$

$$= r^0 P_0^0(\cos\theta)\left[A_0^0 \sin(0) + B_0^0 \cos(0)\right] \qquad \text{(2 continued)}$$

$$+ r^1 P_1^0(\cos\theta)\left[A_1^0 \sin(0) + B_1^0 \cos(0)\right]$$

$$+ r^1 P_1^1(\cos\theta)\left[A_1^1 \sin\phi + B_1^1 \cos\phi\right]$$

$$= B_0^0 + r\cos\theta\, B_1^0 + r\sin\theta\left[A_1^1 \sin\phi + B_1^1 \cos\phi\right] \qquad (2)$$

Converting to rectangular coordinates (see Fig. 1 and coordinate system description) and computing the gradient yields Eqs. 3 & 4.

$$\Phi(n=1) = B_0^0 + yB_1^0 + xA_1^1 + zB_1^1 \qquad (3)$$

$$\vec{H} = -\nabla\Phi = -A_1^1 \vec{a}_x - B_1^0 \vec{a}_y - B_1^1 \vec{a}_z \qquad (4)$$

where $\vec{a}_x, \vec{a}_y,$ and $\vec{a}_z$ are unit vectors.

By inspection $H_x = -A_1^1$, $H_y = -B_1^0$, and $H_z = -B_1^1$.

Similarly, for n = 2 the linear field gradients are included in the series expansion of Eq. 1. (See Ref. 5 for a discussion on the first derivative terms.) E.g., $H_z(n=2) = -B_1^1 - 6A_2^2 \times -3B_2^1 y - \left(6B_2^2 - B_2^0\right) z$

On the midplane of a magnetic dipole oriented in the z direction

$H_x \equiv 0$, $H_y \equiv 0$. Near the midplane of a carefully constructed magnet the minor components of field are small and often can be neglected. Anderson presents another argument for neglecting the minor components.[5] He contends that over the volume of interest the variation in the field ($\vec{H}' = \vec{a}_x H_x' + \vec{a}_y H_y' + \vec{a}_z H_z'$) may be only $1/10^5$ of the field strength ($\vec{H}_0 \approx \vec{a}_z H_z$). The actual field ($\vec{H} = \vec{H}_0 + \vec{H}'$) can then be expanded in the binomial series as follows:

$$|\vec{H}| = \sqrt{(H_0 + H_z')^2 + H_x'^2 + H_y'^2}$$

$$\approx H_0 + H_z' + \frac{H_x'^2 + H_y'^2 + H_z'^2}{2H_0}$$

$$\approx H_0 + H_z' \qquad (5)$$

From these arguments we conclude that it is necessary only to correct the z-component of magnetic field.

Using these simplifying principles, Knight & Erskine in 1965 constructed and tested a set of "Golay" coils designed to control x, y and z derivatives and the "coning" distortion of H_z.[7] With only these controls they achieved a uniformity of $1/10^8$ over a 0.1ml. volume. We followed their example.

THE SELECTION OF ELECTRIC SHIM SHAPES

Due to the reported success of Knight & Erskine at a higher field than ours and with smaller diameter pole pieces than those in our magnet, we decided that first order corrections would also suffice for our magnet. We contemplated the difficulties in 1) carrying out the computations described in the previous section, 2) accurately drawing the contours of the potential function so that "currents of equal magnitude are caused to circulate in each conducting band between two adjacent contour lines," and 3) converting the drawing to a photographic negative or positive suitable for the production of a printed circuit board.

We decided to minimize these difficulties by enlarging the negatives supplied by Knight to a size appropriate to the dimensions of our magnet. Ideally, in scaling between two electromagnets with an iron yoke one would scale all dimensions linearly.* The two significant dimensions in this case are the gap length, g, and the pole face diameter, d.

Taking the ratios of the diameters and gaps of the two magnets yields:

$$d_s/d_k = 11.9/7.9 = 1.51 \quad , \quad g_s/g_k = 2.50/1.00 = 2.50 \qquad (6)$$

Where the subscript, s, stands for Singer, and k, stands for Knight. We

*See Appendix II for laws for scaling for Electromagnetic models.

decided to compromise and make a 200% enlargement of the negatives supplied by Knight.

Knight and Erskine used the "Golay" coils to reduce the x, y and z derivatives of B_z, but abandoned the Golay coil set for reducing the coning effect in favor of two pairs of empirically derived coils 1.25 cm. (0.492 in.) and 2.5 cm. (0.984 in.) in radius.

We tried coil pairs of approximately the same dimensions (1.19 cm and 2.46 cm radius). It turned out that the smaller coil had the more beneficial effect on the field shape.

COIL SYSTEM DESCRIPTION

The coil system consists of two coil holders, a bipolar current source and controller, and interconnecting cables. Each coil holder houses five separately energized coils that are connected electrically in series with identical coils in the other package.

Figure 2 shows the current controller and the batteries on top of the magnet. Figure 3 shows the Author holding the coil holders and Figure 4 is a closer view of the coil holders.

Ist Derivative Coils

The coils whose purpose is to minimize $\partial B_z/\partial x$, $\partial B_z/\partial y$, and $\partial B_z/\partial z$ (See Figures 5-8) were designed following principles outlined by Knight.

The appropriate contours were etched on the front and back faces of 1 oz/ft^2 double-sided printed-circuit-boards (0.00268 in. copper on each side of 0.002 in. N.E.M.A. FR4, total thickness 0.007 in. each board). The copper surface was gold-plated to facilitate making electrical connections.

Appropriate connections through the printed-circuit (P.C.) board connect the front and back, thus eliminating the need for conductors penetrating into the region of interest and introducing undesirable field components. The targets seen in the figures allowed us to align the front and back sides of the boards during fabrication and served as

Fig. 3 Author with Coil-Holders

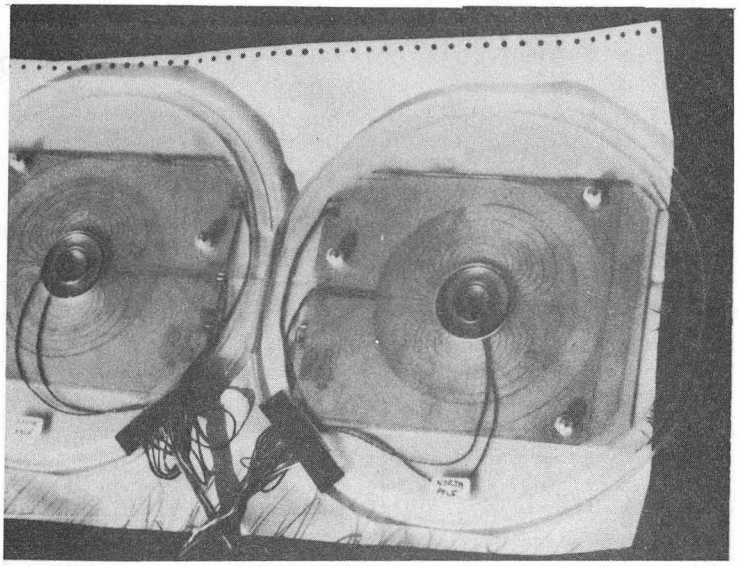

XBB 754-2804

Fig. 4 Coil-Holders

fiducials for mounting the boards in the coil holders. Sheets of Mylar insulation, 0.005 in. thick, are sandwiched between the boards.

Figures 5 and 6 show the front and back faces respectively of an x - derivative coil. Note the current path. I_x^* enters the front face of the printed circuit board (arrow) and circulates in a clock-wise, direction to the center of the spiral where there is a connection to the rear face of the board. The current path continues in a clock-wise (viewed from the front) direction, spiraling outward to a cross-over to the opposite half of the board's rear face where the current is directed in a counter clock-wise direction, circulating to the center of the spiral. Finally, there is a connection to the front face where the current path spirals outward, still in a ccw direction, to the return lead.

The effect of a pair of x - derivative coils is to produce a field aiding the main field for $x>0$ and opposing the main field for $x<0$ (for one polarity of x - derivative coil current, I_x^*) without changing the central field and without introducing other variations.

The y - derivative coils (not shown) are identical to the x- derivative coils except that 1) they are rotated 90^0 about the z - axis with respect to the x - derivative coils; and 2) the connection leads are straight.

A z - derivative coil is shown in Figs. 7 and 8. The current circulation for one coil (both front and back sides) aids the main field

---

*The subscripts x,y,z, C and B identify respectively the currents in x,y and z derivative coils and in the curvature and balance coils.

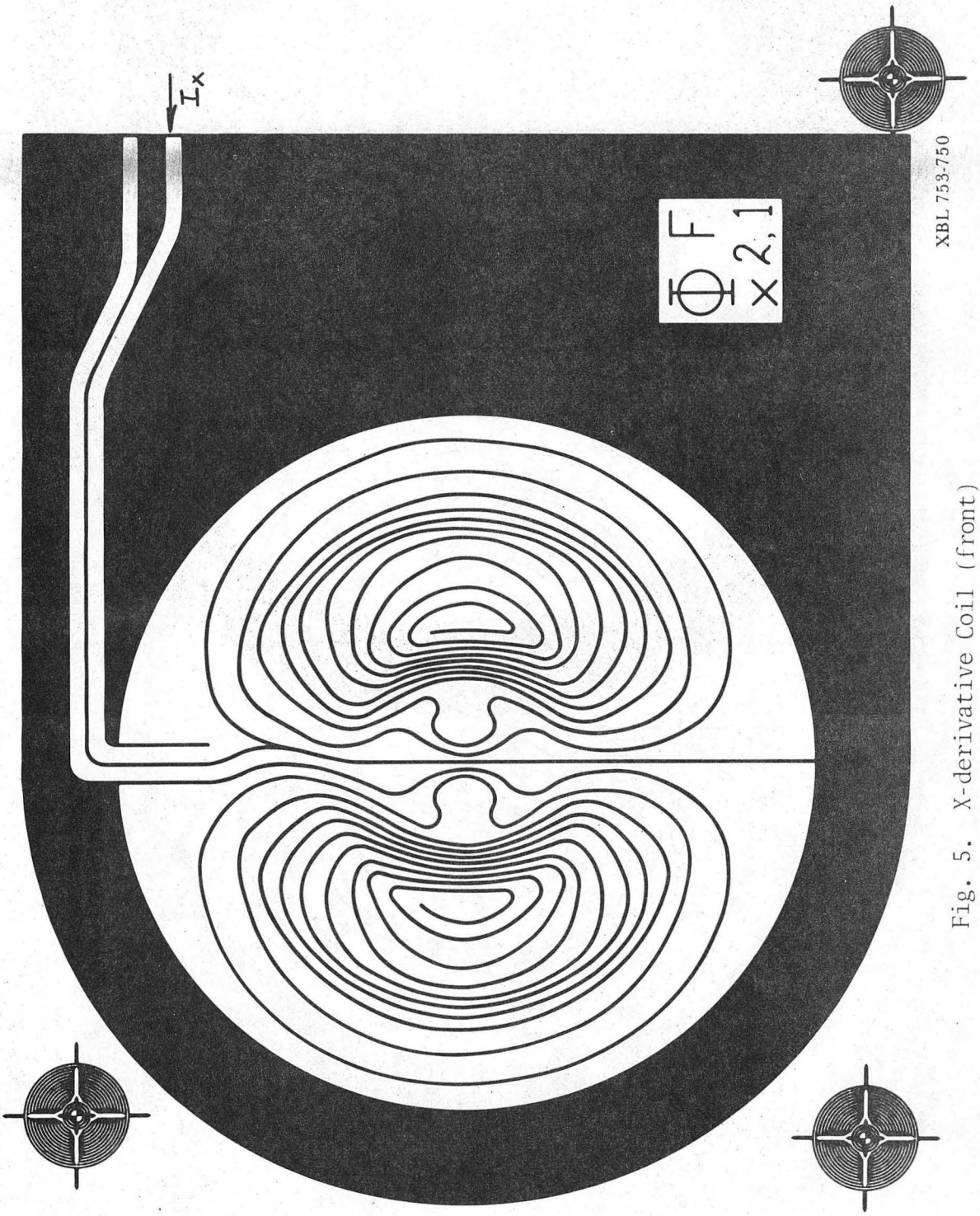

XBL 753-750

Fig. 5. X-derivative Coil (front)

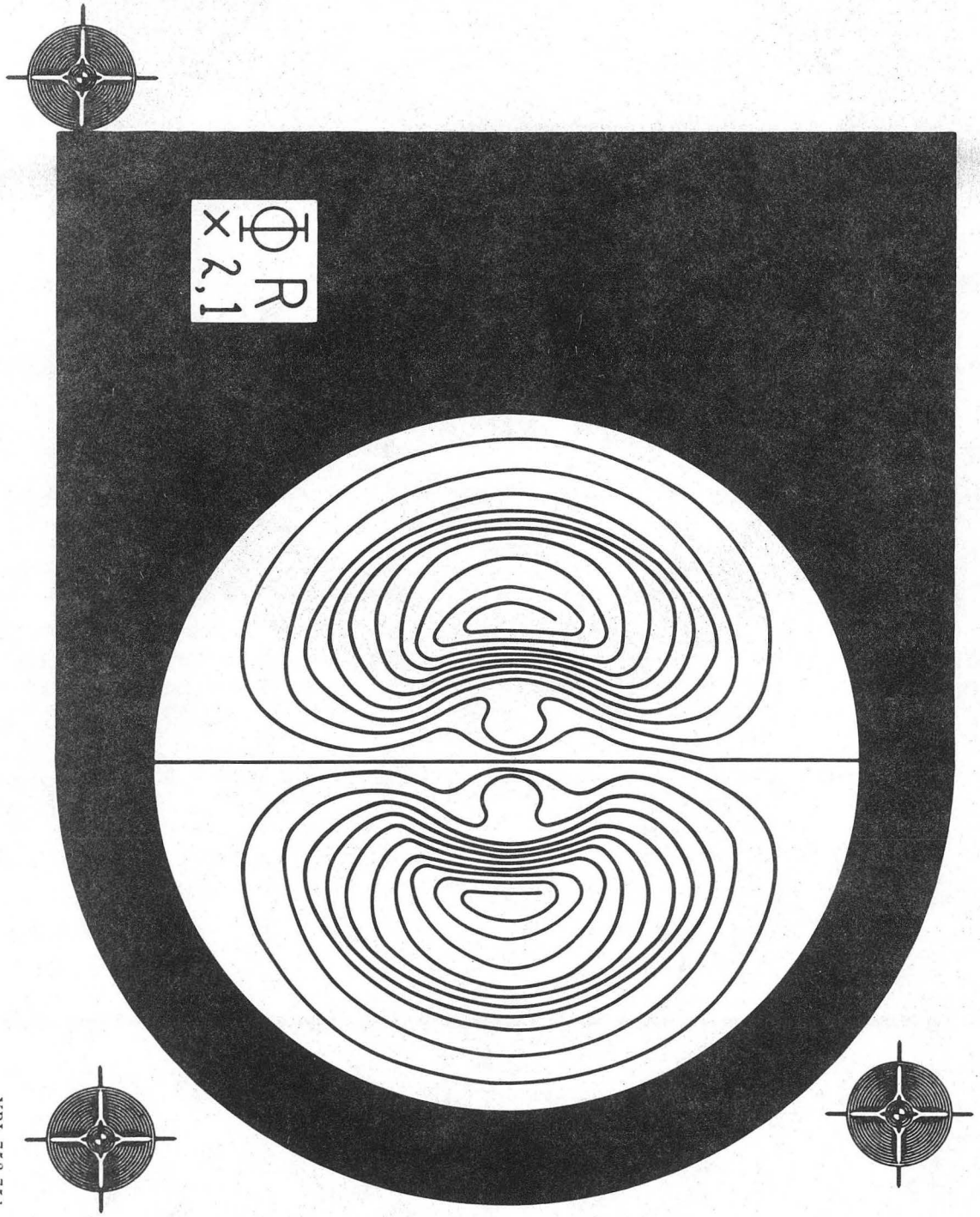

XBL 753-751

Fig. 6. X-derivative Coil (rear)

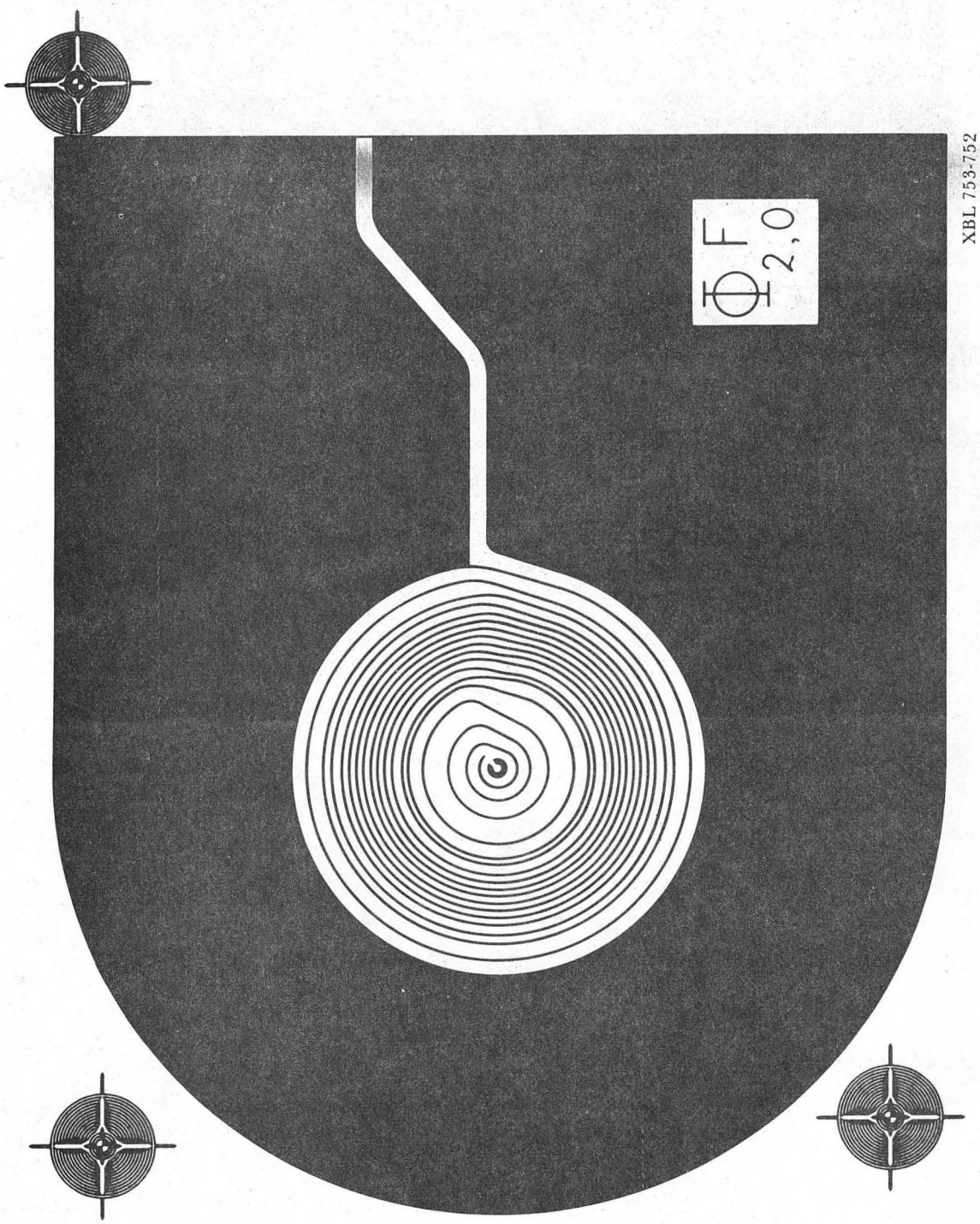

Fig. 7. Z-derivative Coil (front)

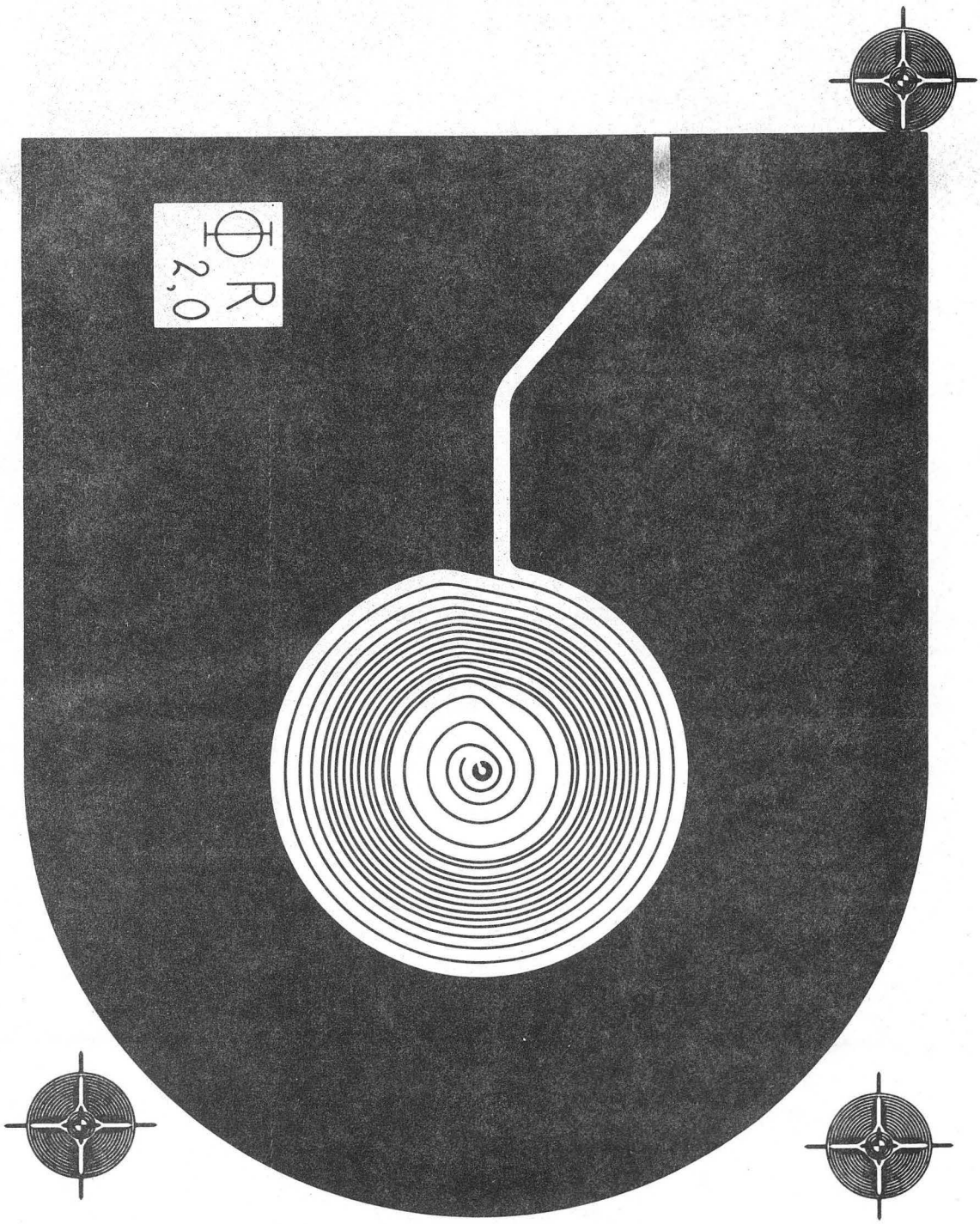

XBL 753-753

Fig. 8. Z-derivative Coil (rear)

while the coil on the opposite pole face opposes the main field thus producing a z - derivative.

Curvature Coils

The two coil pairs that produce fields with second derivatives that are symmetrical about the origin were wound on the lucite forms shown in Fig. 9. Each coil consists of 20 turns of No. 28 magnet wire.

The smaller radius coil-pair is called the curvature coil pair. Its effect is to produce a radial field distribution which will cancel the coning effect (i.e. either the "domed" or "dished" field shape inherent in most electromagnets.[8]) The larger raduis coil-pair is called the "balance" coil-pair. The intended purpose of this pair is to return the central field to its uncompensated value by opposing the field of the curvature coils without introducing significant curvature of its own. Apparently, for the magnet under investigation, the radii of these coil pairs are too near each other to use the balance coil for setting the field level. However, a specified field-magnitude may be held by making a minor adjustment to the main magnet coil current.

Coil-Holders

The coil-holders were machined from lucite (Fig. 10). Nylon screws passing through holes drilled through the centers of the targets on the P.C. boards hold the boards in the coil-holder. The coil-holder then fits tightly over the pole-tip. We had planned to use nylon stanchions

*The subscripts x, y, z, C, and B refer respectively to currents flowing in the x, y, and z derivative coils and curvature, and balance coils.

SUBJECT: CURVATURE COIL FORMS & P.C. BOARD GUIDES

SKETCH

LAWRENCE RADIATION LABORATORY
UNIVERSITY OF CALIFORNIA

DRAWN BY: Don Nelson

DATE: 74 Feb. 11

BUILDING NO. | ROOM NO. | APPROVED BY | DATE

JOB ORDER INFORMATION: JOB NO. | TAG NO. | SERIAL NO. | NO. REQD. | DATE ISSUED | DATE REQD. | DELIVER TO

Material: Plexiglass
Scale: X2
All dimensions (inches)

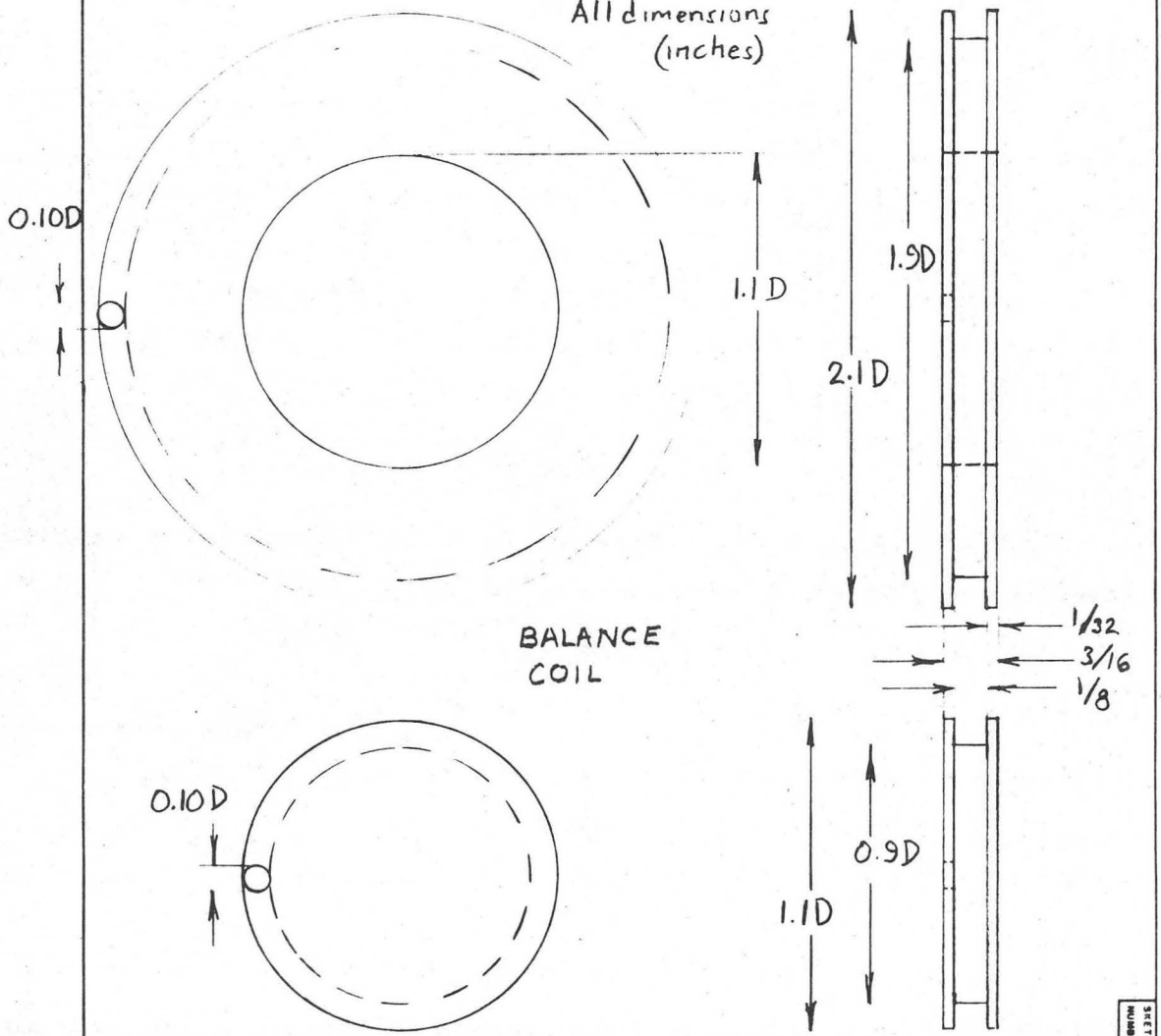

MAKE 2 each to fit Pole Tip Winding Holder '74 Feb1

SKETCH NUMBER

XBL 754-819

Fig. 9 Balance and Curvature Coil Forms Drwg.

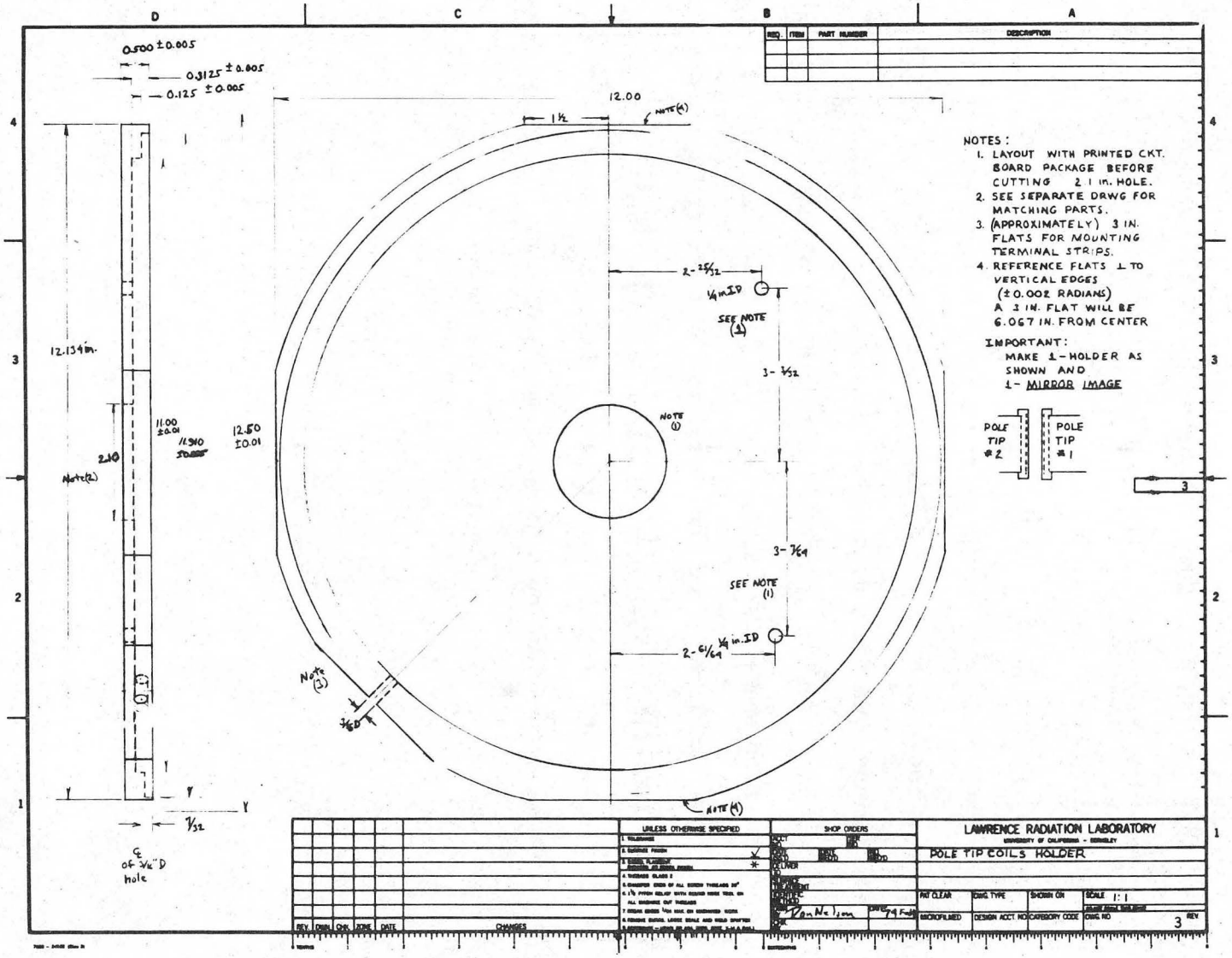

Fig. 10. Coil-Holder Drawing

to keep the coil-holders in place, but they were not needed.

The balance-coils fit holes in the center of the coil-holders. And the balance-coils have holes to accommodate the curvature-coils. Again, we planned to secure the coils with cement but have found the tight fit sufficient to hold the coils in place.

The Bipolar Current Source and Controller

Figure 11 is a schematic of the current controller. The circuitry is a direct copy of the Knight & Erskine control circuit[7] except for one modification. We found with the selection of components specified we drew little current except near the ends of the ranges of the 10-turn potentiometer where its resistance neared that of the limiting resistor.

Larry Crooks modified the circuitry for the curvature and balance current controls to that shown in Figure 11 allowing finer control of those important currents. We intend to modify the remaining controls.

Power is provided by 6 Nickel-Cadmium cells that were purchased from a Surplus Vendor (1.2V, 6 Ampere-Hour, rechargeable cells).

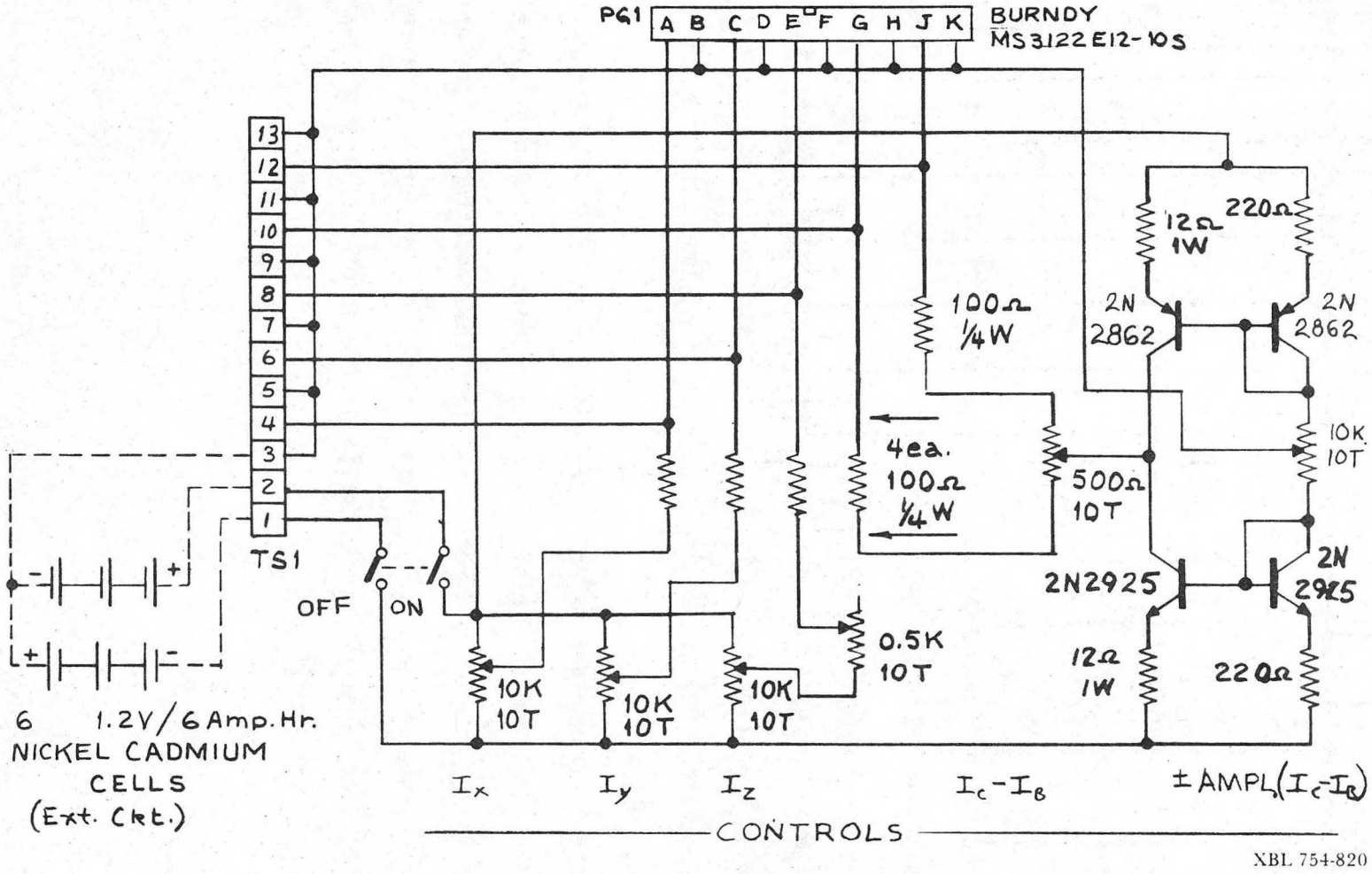

Fig. 11 Current-Controller Schematic

THE MAGNETIC FIELDS PRODUCED BY THE COILS

We measured the magnetic induction contribution of each coil-pair on the 36 point grid described below:

$x = 0, \pm 0.5$ in.

$y = 0, \pm 0.4$ in.

$z = 0, \pm 0.2$ in., -0.4 in.

The measuring-system used for these measurements is described in Appendix III. With the point-coil positioned at each of the grid points, we switched the current-controller on and off with its controls set to maximize one current and zero the remaining currents. We recorded the change in flux-linkage due to each coil at each position. Current was measured with a Hewlett Packard, DC clip-on milliammeter Model No. 428-B, Ser. No. 0995A06747.

The first-derivative coils produce magnetic fields that vary linearly with distance from the origin along one coordinate with negligible variations in the other two directions. The measured effect at the origin of the coordinate system was less than 2.5×10^{-4} G/mA for each of the first-derivative coil-pairs. The normalized effects of the first-derivative coils are summarized in Table I.

Coil	Magnitude of Effect
x-derivative	$\partial B_z/\partial x \div I_x = 1.8 \pm 0.1 \frac{G}{cm}$ per A
y-derivative	$\partial B_z/\partial y \div I_y = 1.9 \pm 0.1 \frac{G}{cm}$ per A
z-derivative	$\partial B_z/\partial z \div I_z = 2.8 \pm 0.15 \frac{G}{cm}$ per A

Table I Normalized Effects of First Derivative Coils

The curvature and balance coil pairs each produce fields that vary approximately as the square of the distance from the origin of our coordinate system. Because these coils are circular, their magnetic effects are readily calculated. For making the calculations we used a Hewlett Packard Programmable Pocket Calculator (HP-65) with a 197 step program that calculates "the magnetic-field of a circle-of-current".[9] Figure 12 shows the measured effects and the calculated effects due to the two coil pairs and their respective "images."

Jackson shows[10] that for the purpose of calculating the magnetic field in a vacuum due to a current distribution adjacent to a material of permeability μ, the material can be replaced by the "image" of the current distribution. If the surface of the material is located at $z' = 0$, and the current distribution is parallel to that surface and located at $z' = z_0$ (i.e., current density = $J(x,y,z' = z_0)$, then the

Fig. 12 Magnetic Effects of the Curvature & Balance Coils

2.5 in. Gap x 11.9 in. Diam. H-Magnet*, Ser. No. 528

Main Coil Current = 0.80 Ampere

$B_z(0,0)$ = 2340 Gauss

Data: '75 Jan. 13 DHN

Drawn: '75 April 28 DHN

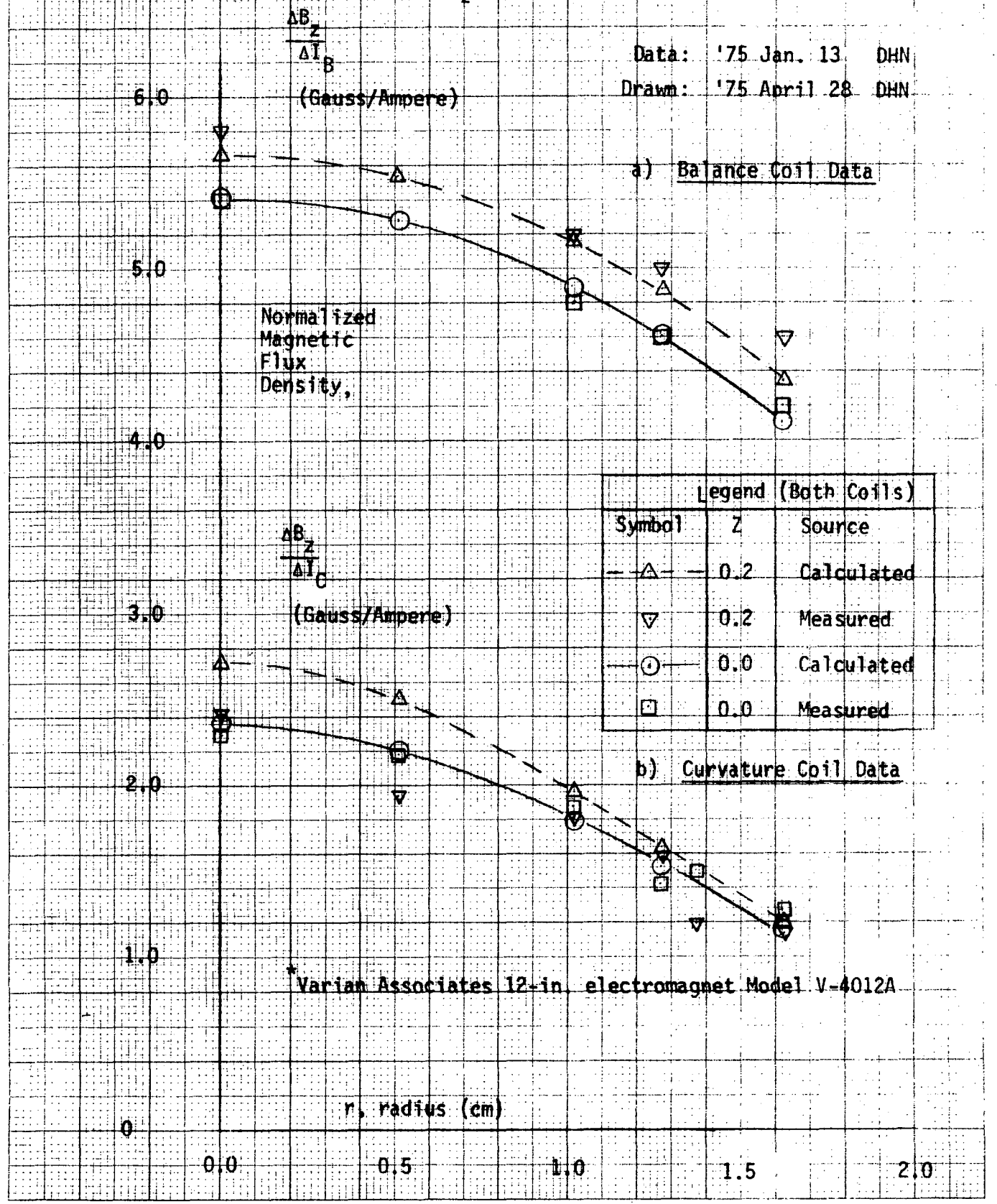

*Varian Associates 12-in. electromagnet Model V-4012A

material can be replaced by the "image" current distribution $J' = \frac{\mu-1}{\mu+1} J(x,y,z' = -z_0)$. For the calculated effects shown in Fig. 12, we added the effects of the circles of current represented by each coil to the effects of the image circles that represent the two pole-tips. A total of six circles of current were included in the calculations for each coil pair. The effect, in the region of interest, of the image from the pole-tip farthest from the coil was less than 5.0% of the total effect shown in Fig. 12. Images of the images were considered and were found to have effects less than 0.5% of the total effect, so the effects of the second and higher images were not included in the calculations.

Figure 13 summarizes three sets of average-radial-profile data for the magnet. Curves 1 and 2 represent the approximate field shape adjustment required in order to flatten the field near the origin of our coordinate system (i.e., the negative of the measured radial distributions of B_z). Curve 1 was derived from a plot of the magnetic field in the median plane of our magnet made at Varian Associates in October 1960.[11] The 1960 data measured with $B_z(0,0) = 9.4$ kG were scaled to $B_z(0,0) = 2.34$ kG by multiplying by the ratio of the fields at the origin. Curve 2 summarizes the July 1973 magnetic field measurements referred to earlier.[2]

Curve 3 in Fig. 13 summarizes the measured magnetic-field shape which optimized the NMR Spin-Echo signal as described in the next section.

Fig. 13 Average-Radial-Profiles of Magnetic Induction
2.5 in. Gap x 11.9 in. Diam. H-Magnet*, Ser. No. 528
Main Coil Current = 0.30 Ampere
$B_z(r=0)$ = 2340 Gauss

Drawn: '75 April 29 DHN

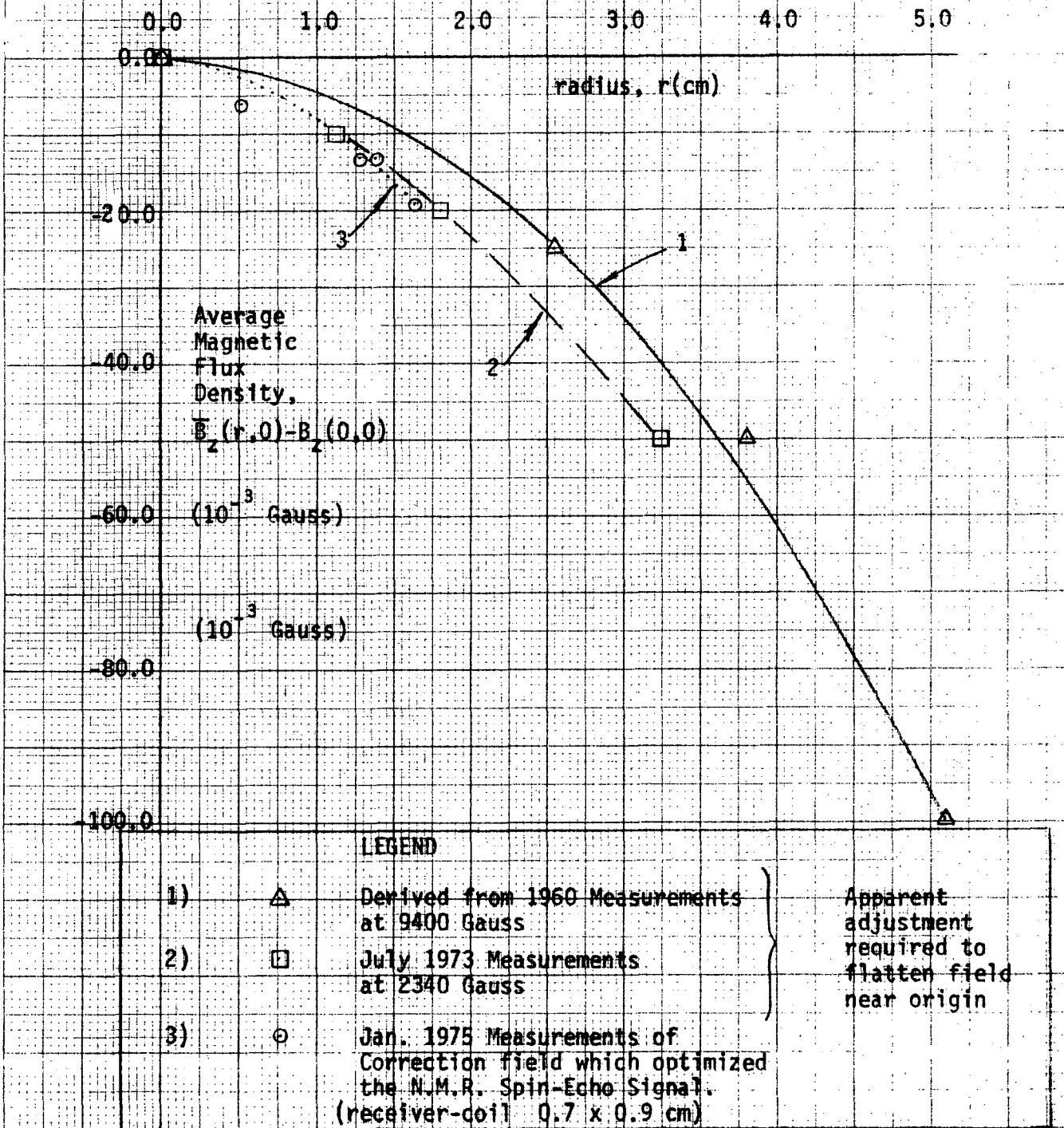

*Varian Associates 12-in. electromagnet Model V-4012A

IMPROVEMENT IN HOMOGENEITY BASED ON N.M.R. SPIN-ECHO SIGNALS

Farrar and Becker[†12] define T_2^*, the free-induction-decay time-constant in the presence of magnetic-field inhomogeneity, by Eq. 7.

$$1/T_2^* = 1/T_2 + \gamma \Delta B_0/2 \qquad (7)$$

$T_2 \equiv$ transverse or spin-spin relaxation time.
(For water in equilibrium with the oxygen in the atmosphere at 25^0 C : $T_2 \approx 2$ sec)[13]

$\gamma \equiv$ magnetogyric ratio (For Hydrogen $\gamma = 2.675 \times 10^4$ (radians/sec per Gauss)

$\Delta B_0 \equiv$ inhomogeneity in the region of interest of the D.C. magnetic-flux-density. (Gauss)

A measure of T_2^* is a sensitive indication of the field homogeneity for $T_2^* << 2$ sec.

Solving for ΔB_0 using the values above for T_2 and γ yields Eq. 8.

$$\Delta B_0 = \frac{2.0}{\gamma} \times \frac{T_2 - T_2^*}{T_2 T_2^*} = 3.75 \times 10^{-5} \frac{2.0 - T_2^*}{T_2^*} \quad \text{(Gauss)} \qquad (8)$$

[†]Farrar and Becker use ΔH_0 which is numerically equal to ΔB_0 in a vacuum in the electromagnetic system of units (emu).

L. E. Crooks (Fig. 14) supervised the N.M.R. spin-echo measurements used for the calculation of T_2^*. The N.M.R. spin-echo measurement system is described in detail elsewhere.[14] The N.M.R. probe used for these measurements (Figs. 15 and 16) was designed and fabricated by Crooks. The 0.7 cm diameter x 0.9 cm long receiver coil was positioned at the origin of our coordinate system with its axis along the x-axis. The saddle shaped transmitter coil[15] (2.5 cm diameter x 5.0 cm long) was positioned with its axis along the y-axis of our coordinate system.

Our procedure was to vary the current in each of the electric-shim coil-pairs while observing the spin-echo signal for an increase in signal width. When we varied the x, y, and z gradient coil currents, we only observed decreases in the signal width for both polarities of current. We conclude that the first derivatives at the origin were negligible for the uncorrected field.

Figure 17 is a record of the improvement we observed in field homogeneity with various combinations of correction coil currents. The half-amplitude width of the envelope of the signal is a measure of T_2^*. Table II summarizes T_2^* and the respective values of ΔB_0 for the four cases shown in Fig. 17.

Fig.	T_2^* (msec.)	ΔB_0 (Gauss)	$\Delta B_0/B_0$ (per unit)
17 a.	22	3.4×10^{-3}	1.4×10^{-6}
17 b.	100	7.1×10^{-4}	3.0×10^{-7}
17 c.	144	4.8×10^{-4}	2.1×10^{-7}
17 d.	220	3.0×10^{-4}	1.3×10^{-7}

Table II Homogeneity Derived from T_2^*.

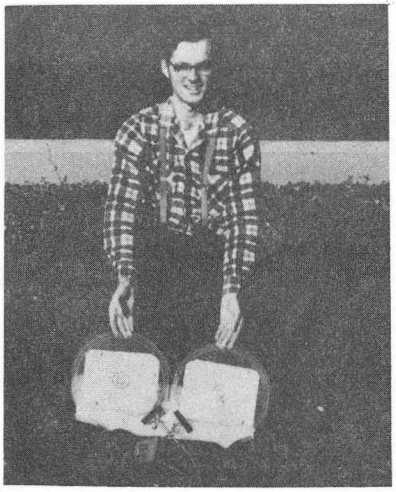

Fig. 14 Larry Crooks with Coil-Holders

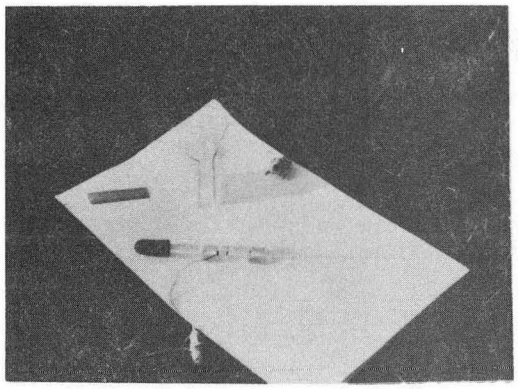

Fig. 15 NMR Probe (Assembled)

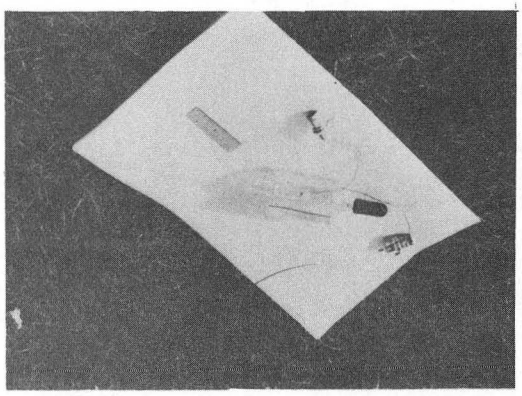

Fig. 16 NMR Probe (Sample & Receiver removed from transmitter

XBB 754-2911

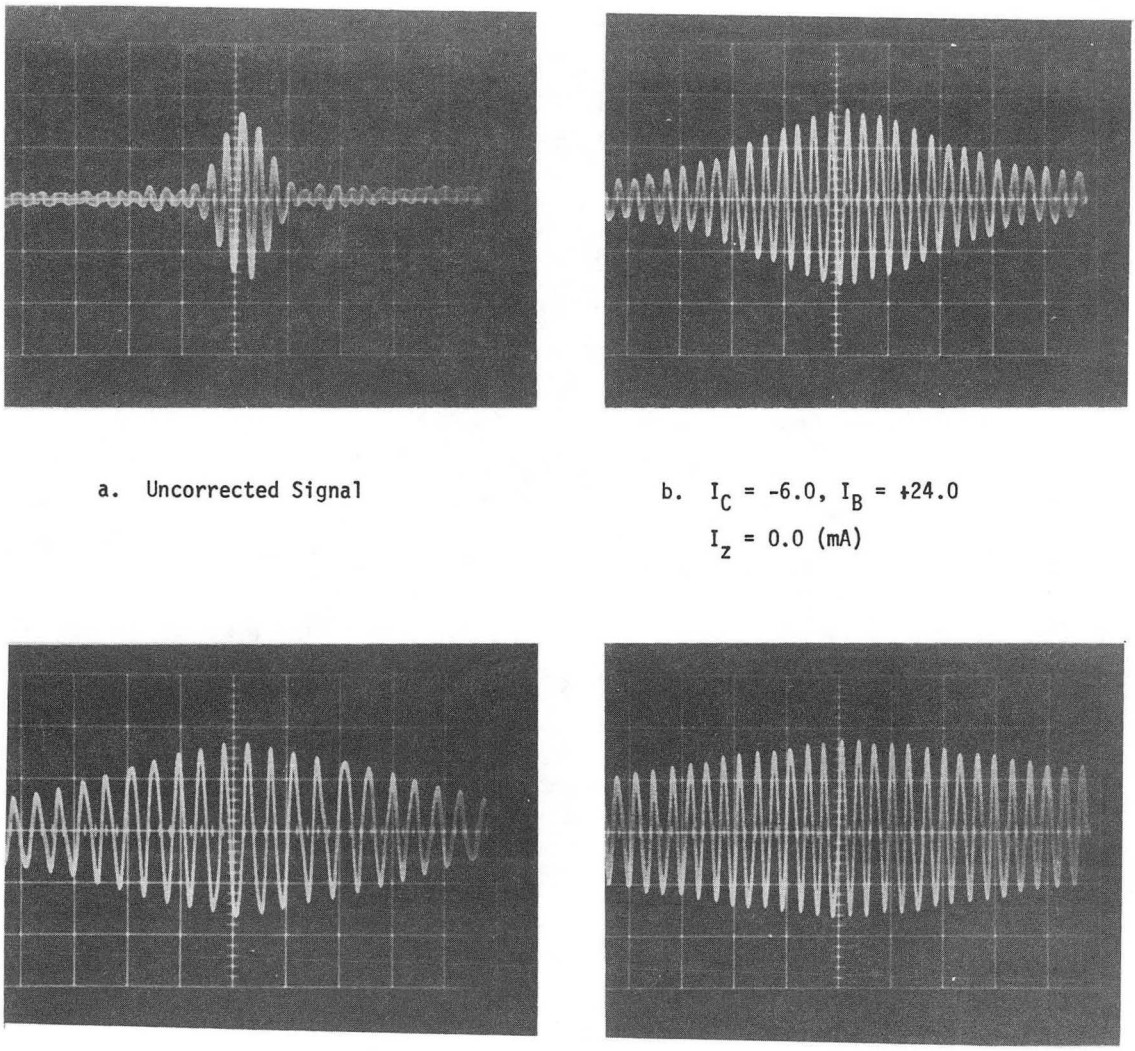

a. Uncorrected Signal

b. I_C = -6.0, I_B = +24.0
I_z = 0.0 (mA)

c. I_C =-6.0, I_B = +24.0
I_z = 1.5 (mA)

d. I_C = 17.2, I_B =-0.3
I_z = 1.4 (mA)

XBB 754-3301

Fig. 17 Effects of Selected Current Distributions on the Period of N.M.R. Spin-Echo Signals

I_m = 0.30 A., $B_z(0,0)$ = 2340.0 Gauss, Sweep Rate = 20 msec/div., Vert. Sens. = 1V/cm.

A study of Fig. 17 and Table II leads to the conclusion that most of the improvement was due to the circular-correction-coil currents I_C & I_B (A factor of 4.5 in signal width as determined from Fig. 17b). Another factor of two improvement was achieved by adjusting the z - derivative current, I_z (Fig. 17C). Once again no improvement was observed when we varied either I_x or I_y.

The maximum signal width was observed (Fig 17d) after we reversed the polarity of both I_c and I_B and readjusted the relative magnitudes of these currents. This effect was expected, because the curvature and balance coils are connected in series opposition. (When $I_c > 0$, and the curvature-coil-pair produces a "domed" field; $I_B \leq 0$, and the balance-coil pair produces a "dished" field, or none at all).

Equation 9 describes the envelope of a theoretical model of free induction decay signals that has been considered valid in a gradient field.[1,14,16]

$$V(\tau) = K \frac{\sin(\gamma g a \tau)}{\gamma g a \tau} \qquad (9)$$

V ≡ Amplitude (Volts).

K ≡ Constant that includes the magnitude of the total magnetization Vector and the gain of the electronics.

γ ≡ Magnetogyric ratio, 2.675×10^4 (radians/sec per Gauss).

τ ≡ Time measured from the location of the apex of the curve. (Sec.)

g ≡ Gradient (Gauss/cm).

2a ≡ Effective length of the N.M.R. receiver coil. (cm.)

$V(\tau = 0) = K$; the expression K sin x/x has its second maximum, of magnitude 0.22K, at x = 4.49 radians. On close examination of the signals shown in Figs. 17a and b, we notice that the envelopes of the signals do have second

maximums with amplitudes approximately 1/5 of the $\tau = 0$ amplitude.

We estimated the location of the second maximums and calculated ga for the two cases. (See Table III.) The values for ga are in rough agreement with the values of ΔB_0 based on Eq. 7. I have not found a precise definition of the "inhomogeneity of the magnetic-flux-density" (ΔB_0 in Eq. 7).

Fig.	Location of 2nd peak (sec.)	$ga = \frac{4.49}{\gamma T}$ (Gauss)	B_0 (Table 1) (Gauss)
17a	$\pm$ 32 x 10^{-3}	5.3 x 10^{-3}	3.4 x 10^{-3}
17b	$\pm$ 86 x 10^{-3}	1.96 x 10^{-3}	7.1 x 10^{-4}

Table III Comparison of Homogeneities
Based on Eqs. 7 & 9

DISCUSSION

A system of coils is a convenient and versatile method of increasing the volume of homogeneous field in an electromagnet. In less than two hours of tuning and evaluation, we achieved the results recorded by the photos in Fig. 17. The spin-echo signal duration, T_2^*, was increased 10 times, from 0.022 to 0.220 seconds.

We expect this system to provide satisfactory optimization over a wide range of field levels and sample sizes in the magnet for which it was designed. In addition, the system probably could be adapted to other electromagnets or permanent-magnets with cylindrical pole tips.

Further improvements in the quality of N.M.R. signals in our magnet probably can be achieved by spinning the sample about its axis.[8,17]

As noted earlier, most of the observed improvements were due to the circular currents. If one wanted to try to improve the quality of his N.M.R. display in another magnet, he might 1) Wind several circular coil-pairs of different radii, 2) Attach the coil pairs to the pole-faces of his magnet, symmetrically with respect to both the magnet and his N.M.R. sample, and 3) Examine the variation of his N.M.R. display as a function of the coil currents.

Appendix I

SOLUTION OF LAPLACE'S EQUATION IN SPHERICAL COORDINATES[6]

For a current free region the magnetic scalar potential, Φ, satisfies Laplace's equation. Laplace's equation in spherical coordinates is given by Eq. 1. (A1.01).[19]

$$\nabla^2\Phi = \frac{1}{r^2}\frac{\partial}{\partial r}\left(r^2\frac{\partial\Phi}{\partial r}\right) + \frac{1}{r^2\sin\theta}\frac{\partial}{\partial\theta}\left(\sin\theta\frac{\partial\Phi}{\partial\theta}\right) + \frac{1}{r^2\sin^2\theta}\frac{\partial^2\Phi}{\partial\phi^2} = 0 \quad \text{(A1.01)}$$

A standard method for solving partial differential equations is to assume a product solution of the form of Eq. 2, where R, P, and Q are each functions of a single variable as indicated.

$$\Phi(r,\theta,\phi) = R(r)P(\theta)\,Q(\phi) \quad \text{(A1.02)}$$

Substituting Eq. 2 into Eq. 1 and rearranging produces Eq. 3.

$$\frac{\partial^2 Q}{\partial\phi^2}/Q = -\frac{\sin^2\theta}{R}\frac{\partial}{\partial r}\left[r^2\frac{\partial R}{\partial r}\right] - \frac{\sin\theta}{P}\frac{\partial}{\partial\theta}\left[\sin\theta\,\frac{\partial P}{\partial\theta}\right] \quad \text{(A1.03)}$$

Now the expression on the left side of Eq. 3 is a function of ϕ only, while the expression on the right side of Eq. 3 is a function of the variables r and θ. These expressions can be equal to each other for arbitary values of the independent variables r, θ, and ϕ only if the

expressions are independent of r, θ and ϕ (i.e. are constant). Setting the constant equal to $-m^2$ gives us Eq. 4.

$$\frac{d^2Q}{d\phi^2} /Q = -m^2 \qquad \text{(A1.04)}$$

Substituting Eq. 4 into Eq. 3 and rearranging produces Eq. 5.

$$\frac{1}{R} \frac{\partial}{\partial r} \left[r^2 \frac{\partial R}{\partial r} \right] = \frac{-m^2}{\sin^2\theta} - \frac{1}{P\sin\theta} \frac{\partial}{\partial \theta} \left[\sin\theta \frac{\partial P}{\partial \theta} \right] \qquad \text{(A1.05)}$$

The expression on the left is a function of r while the expression on the right is a function of θ, so for equality to hold the expressions must be constant. Setting the constant equal to $\ell(\ell+1)$ produces Eq. 6 and Eq. 7.

$$\frac{1}{R} \frac{d}{dr} \left[r^2 \frac{dR}{dr} \right] = \ell(\ell+1) \qquad \text{(A1.06)}$$

$$\frac{m^2}{\sin^2\theta} + \frac{1}{P\sin\theta} \frac{d}{d\theta} \left[\sin\theta \frac{dP}{d\theta} \right] = -\ell(\ell+1) \qquad \text{(A1.07)}$$

Making the substitutions $x = \cos\theta$, $dx = -\sin\theta d\theta$, and $\sin^2\theta = 1-\cos^2\theta = 1-x^2$ in Eq. 7 yields Eq. 8

$$\frac{d}{dx}\left[(1-x^2)\frac{dP}{dx}\right] + \left[\ell(\ell+1) - \frac{m^2}{1-x^2}\right] P = 0 \; ; \; x = \cos\theta \qquad \text{(A1.08)}$$

Equations 4, 6 and 8 are plain differential equations which have the solutions shown in Eqs. 9.[20,21]

$$Q = A'\sin m\phi + B'\cos m\phi \qquad \text{(A1.09a)}$$

$$R = C'r^{\ell} + D' r^{-(\ell+1)} \qquad \text{b)}$$

$$P = E'P_{\ell}^{m}(x) + F'Q_{\ell}^{m}(x) \quad ; \; x = \cos\theta \qquad \text{c)}$$

Substituting the equations 9 into Eq. 2 yields the most general solution to Laplace's Equation (Eq. 10).

$$\Phi(r,\theta,\phi) = \left[A'\sin m\phi + B'\cos m\phi\right]\left[C'r^{\ell} + D'r^{-(\ell+1)}\right]$$

$$\left[E'P_{\ell}^{m}(\cos\theta) + F'Q_{\ell}^{m}(\cos\theta)\right] \qquad \text{(A1.10)}$$

If the origin is included in the problem D = 0. Similarly, if the polar axis is included in the problem F = 0. The problem we are concerned with in this work includes both restrictions so the solution reduces to that shown in Eq. 11.

$$\Phi(r,\theta,\phi) = r^{\ell}P_{\ell}^{m}(\cos\theta)\left[A_{\ell}^{m}\sin m\phi + B_{\ell}^{m}\cos m\phi\right] \qquad \text{(A1.11)}$$

P_ℓ^m is called an Associated Legendre Polynomial of the first kind, order m, degree ℓ. The polynomials in cosθ can be determined by recursion formulas. The first few polynomials are listed in Table I.[21]

$$P_0(z) = 1$$
$$P_1(z) = z = \cos\theta$$
$$P_1^1(z) = (1 - z^2)^{\frac{1}{2}} = \sin\theta$$
$$P_2(z) = \tfrac{1}{2}(3z^2 - 1) = \tfrac{1}{4}(3\cos 2\theta + 1)$$
$$P_2^1(z) = 3(1 - z^2)^{\frac{1}{2}}z = \tfrac{3}{2}\sin 2\theta$$
$$P_2^2(z) = 3(1 - z^2) = \tfrac{3}{2}(1 - \cos 2\theta)$$
$$P_3(z) = \tfrac{1}{2}(5z^3 - 3z) = \tfrac{1}{8}(5\cos 3\theta + 3\cos\theta)$$
$$P_3^1(z) = \tfrac{3}{2}(1 - z^2)^{\frac{1}{2}}(5z^2 - 1) = \tfrac{3}{8}(\sin\theta + 5\sin 3\theta)$$
$$P_3^2(z) = 15(1 - z^2)z = \tfrac{15}{4}(\cos\theta - \cos 3\theta)$$
$$P_3^3(z) = 15(1 - z^2)^{\frac{3}{2}} = \tfrac{15}{4}(3\sin\theta - \sin 3\theta)$$
$$P_4(z) = \tfrac{1}{8}(35z^4 - 30z^2 + 3) = \tfrac{1}{64}(35\cos 4\theta + 20\cos 2\theta + 9)$$
$$P_4^1(z) = \tfrac{5}{2}(1 - z^2)^{\frac{1}{2}}(7z^3 - 3z) = \tfrac{5}{16}(2\sin 2\theta + 7\sin 4\theta)$$
$$P_4^2(z) = \tfrac{15}{2}(1 - z^2)(7z^2 - 1) = \tfrac{15}{16}(3 + 4\cos 2\theta - 7\cos 4\theta)$$
$$P_4^3(z) = 105(1 - z^2)^{\frac{3}{2}}z = \tfrac{105}{8}(2\sin 2\theta - \sin 4\theta)$$
$$P_4^4(z) = 105(1 - z^2)^2 = \tfrac{105}{8}(3 - 4\cos 2\theta + \cos 4\theta)$$

Table AI-I

Associated Legendre Functions

Appendix II

SCALING LAWS FOR ELECTROMAGNET MODELS

The laws of scaling are covered under the general theory of Modeling.[22] The scale factors which can be chosen arbitrarily are called fundamental scale factors. The number of fundamental scale factors is identical with the number of fundamental dimensions necessary for a complete dimension system. Four fundamental dimensions form a complete dimension system for the field of electro magnetism exclusive of thermal phenomena.

We are interested in scaling length, and because of the non-linear nature of ferromagnetic materials, we want magnetic induction the same in the model as in the full scale magnet. For simplicity, we choose the conductor material and geometrical shape the same in the model as in the full scale magnet.

Equations 1 - 4 constitute a sufficient set of independent modeling relations for an electro magnet that contains ferromagnetic material.

$$B_m(H_m) = B(H) \qquad \text{(A2.01)}$$

$$\rho_m = \rho \qquad \text{(A2.02)}$$

$$d_m = d \qquad \text{(A2.03)}$$

$$\ell_m = k\ell \qquad \text{(A2.04)}$$

m Subscript denoting a model parameter

B Magnetic induction (Eq. 1 emphasizes the fact that B depends on the magnetic field intensity, H

ρ Resistivity of the current carrying conductor

d Density of the material involved

ℓ Linear dimension (e.g. pole tip diameter, distance between pole tips, etc.).

k Linear scale factor.

With these choices of fundamental scaling factors the dependent scaling factors can be derived by dimensional analysis. Some of the interesting dependent scaling factors are derived below.

It is interesting to note that although the power in the model varies linearly with the scaling factor, k, the power density in the model is proportional to the reciprocal of k^2. Under the above assumptions cooling problems control the lower limit of the scale factor of an electro magnet model.

Area and Volume	$A_m = k^2 A \ , \ V_m = k^3 V$
Magnetic Field Intensity	$H_m = \frac{B_m}{\mu} = \frac{B}{\mu} = H$
Current Density	$J_m = \nabla x H_m = \frac{1}{k} \nabla x H = \frac{J}{k}$
Current	$I_m = J_m A_m = \frac{J}{k} k^2 A = kI$
Resistance	$R_m = \frac{\rho_m \ell_m}{A_m} = \frac{\rho k \ell}{k^2 A} = \frac{R}{k}$
Power	$P_m = I_m^2 R_m = k^2 I^2 \frac{R}{k} = kP$
Power density	$\frac{P_m}{V_m} = \frac{kP}{k^3 V} = \frac{P}{k^2 V}$
Weight	$W_m = d_m V_m = dk^3 V = k^3 W$

Appendix III

COIL/INTEGRATOR MAGNETIC FIELD MEASUREMENT SYSTEM

The January 1975 measurements of the 12-inch Varian Magnet, Model No. V-4012A, Ser. No. 529 were made with the equipment listed in Table A III - I.

The Electronic Integrator (see Fig. A III - 1) is a design that reflects many years of experience with the development of electronic integrators at Lawrence Berkeley Laboratory. "This design incorporates careful guarding, isolation, and simplification of the summing-junction.

DEVICE	IDENTIFICATION AND NOTES
Electronic Integrator	LBL Model '71, Ser. No. 8, LBL Drwg. No. 6V1763, R7 = 51.1 x 10.0^{3} (Ω) (nominal) C1 = 0.20 x 10.0^{-6} (F), (nominal) Output Attenuator Setting = 582
Point-Coil	LBL, Coil No. B-145, Area, nA = 5370 cm^{2} Resistance, Rcoil = 2.30 x 10.0^{3} (Ω) (at 25^{o}C)
Flux Standard	LBL SLFS No. 39, LBL Drwg. No. 5V4994 Φ = 0.00952 (Volt-Seconds)
x-y Plotter	Mosely Model No. 7000-AR, Ser. No. 709-01034
Bias Box	LBL Drwg. No. 5V8032
D. C. Milliammeter	Hewlett Packard Clip-on, Model No. 428B, Ser. No. 0995A06747
Positioner	LBL 2-Dimensional, Precision Lead-Screws
Coil Positioner	LBL 16 in. Linear Positioner

Table A III-I Equipment List

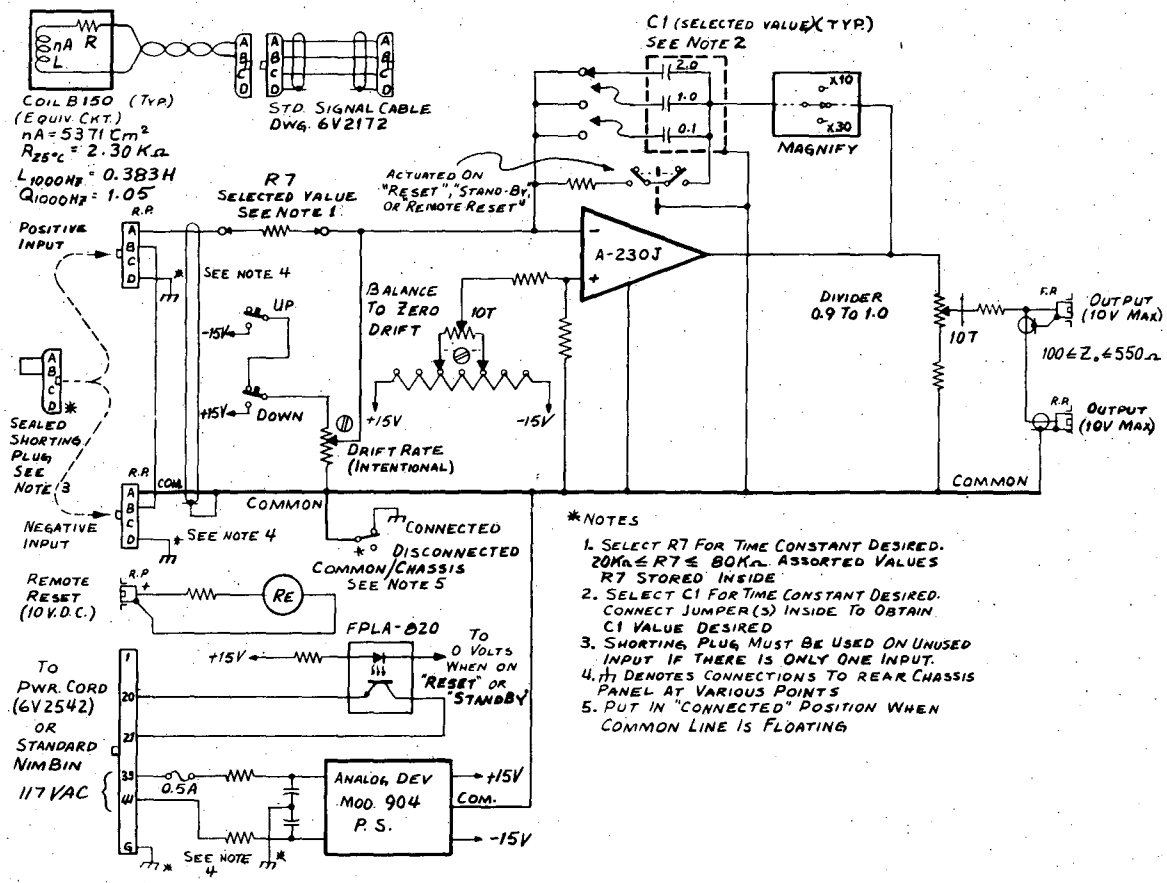

XBL 754-1008

Fig. A III - 1, Electronic Integrator Block Diagram

We use Teflon dielectric capacitors to achieve low leakage and low temperature coefficient of capacitance."[23]

Figure AIII-2 shows the point-coil positioned in the magnet gap. The point-coil is a cylindrical coil with dimensions chosen such that the flux linking the coil is approximately proportional to the magnetic induction at the geometrical center of the cylinder.[24] The coil is enclosed in an epoxy cube 1.20 cm on a side.

The Flux-Standard is a portable, secondary-standard of $\int$Vdt used for determinining the operational time constant of the integrator. "A reproducible $\int$Vdt pulse is generated by reversing the magnetization of a temperature-controlled, temperature-compensated toroidal-core transformer."[25]

The core of ribbon-wound Deltamax is normally saturated in one direction by current in the primary winding. When the primary current is reversed, an accurately reproducible flux change links the output winding (secondary). In 1967, Macondray claimed accuracies of 0.03% for the $\int$Vdt pulses generated by the flux-standards.[25] Six individual units have been calibrated several times. The results are in agreement with Macondray's claims.[26]

The point-coil was positioned on grid points in the magnet coordinate system with the positioner shown in Fig. AIII-3. A 16-in. linear coil positioner was mounted on a 2-dimensional positioning frame, so the coil could be extended into the magnet gap as shown in Fig. AIII-2.

For measuring separate and combined effects of the electric-shim coil-currents, we positioned the coil and measured changes in flux-linkage as we switched the electric-shim current controller on and off.

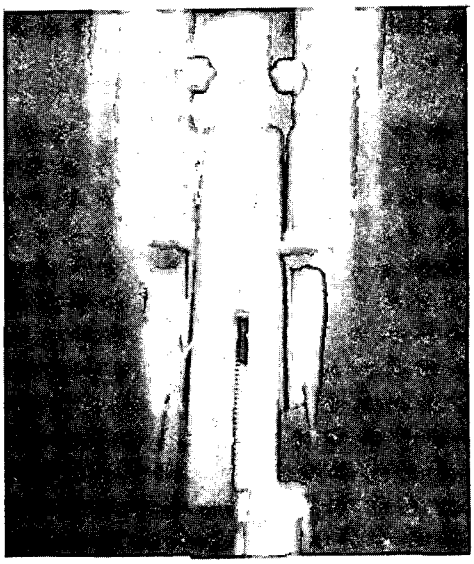

Fig. A III - 2 Magnet Gap with Coil-Holders Installed
(Field-Measurement-Coil in Gap)

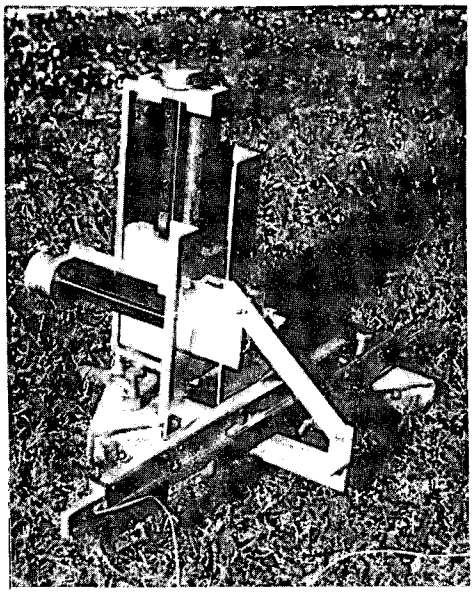

Fig. A III - 3 Three-Dimensional Coil-Positioner
for Magnetic Measurements

XBB 754-3181

REFERENCES

1. T. P. Grover and J. R. Singer, "NMR Spin-Echo Flow Measurements," J. Appl. Phys. 42, 3 (1971).

2. D. H. Nelson, "Magnetic Measurements of a 12 in. Diameter Laboratory Electromagnet (Varian V-4012A, Ser. No. 528)" Lawrence Berkeley Laboratory Magnetic Measurements Engineering Note MT-249, UCID-3740 (1973).

3. F. A. Nelson, "Means and Apparatus for Improving the Homogeneity of Magnetic Fields," U. S. Patent No. 2,858,504 (1955).

4. M. F. E. Golay, "Field Homogenizing Coils for Nuclear Spin Resonance Instrumentation," Rev. Sci. Inst. 29, 313 (1958).

5. W. A. Anderson, "Electric Shims" N.M.R. and E.P.R. Spectroscopy, The Macmillan Company, (1960), Chapter 13.

6. J. R. Whinnery, University of California, Dept. of Electrical Engineering and Computer Science, Class notes EE-210A, (1974).

7. S. A. Knight and R. L. Erskine, "Conversion of a Varian 40 Mc/s High Resolution Nuclear Magnetic Resonance Spectrometer to 80 Mc/s Operation," J. Sci. Instrum., 42, 669, (1965).

8. F. A. Nelson, "Instrumentation of High Resolution N.M.R.," N.M.R. and E.P.R. Spectroscopy, The MacMillan Company, (1960), Chapter 6.

9. C. G. Dols, "The Magnetic Field of a Circle of Current," To be submitted to the HP-65 Users' Library, Hewlett-Packard Company, 19310 Pruneridge Ave., Cupertino, CA. 95014,(1975).

10. J. D. Jackson, "Classical Electrodynamics," John Wiley & Sons, Inc., (1962), P167.

11. R. Vaughn, "Magnet Field Plot No. 1402," Varian Associates, Palo Alto, CA. (1960).

12. T. C. Farrar and E. D. Becker, "Pulse and Fourier Transform N.M.R.," Academic Press, (1971).

13. H. Y. Carr and E. M. Purcell, Phys. Rev. 94,630 (1954).

14. T. P. Grover "Nuclear Magnetic Resonance Spin-Echo Flow Measurements," P.H.D. Thesis University of California, Berkeley, CA. (1971).

15. D. M. Ginsberg and M. J. Melchner, "Optimum Geometry of Saddle Shaped Coils for Generating a Uniform Magnetic Field," Rev. Sci. Inst. 41, 122 (1970).

References - Continued

16. J. R. Singer, University of California, Dept. of Electrical Engineering and Computer Science, Private Communications (1975).

17. R. Vaughn, Varian Associates Palo Alto, CA. Private Communication (1975).

18. O. C. Morse and J. R. Singer, "Blood Velocity Measurements in Intact Subjects," Science 170, 440 (1970).

19. S. Ramo, J. R. Whinnery, and T. Van Duzer, "Fields and Waves in Communications Electronics," John Wiley & Sons Inc., (1965).

20. J. D. Jackson, "Classical Electrodynamics," John Wiley & Sons Inc., (1962), Chapter II.

21. J. A. Stratton, "Electromagnetic Theory," McGraw-Hill, (1941), Appendix 4.

22. O. W. Eshback, "Handbook of Engineering Fundamentals," John Wiley & Sons Inc., 2nd Ed. (1952) Section 3.

23. C. G. Dols "A Computer Controlled, 3-D, Magnetic Field Mapping System," Proceedings of the Fourth International Conference on Magnet Technology, Brookhaven National Laboratory, Upton, N. Y. (1972). (Also published as Lawrence Berkeley Laboratory, Report LBL-1311).

24. C. G. Dols and P. G. Watson, "Search Coil Parameters," Lawrence Berkeley Laboratory Magnet Measurements Engineering Note MT-69B, UCID-1602-1 (Rev. 1968).

25. F. W. Macondray "The'Square Loop' Flux. Standard: A Precision Pulse Gnerator," Proceedings of the Second International Conference on Magnet Technology, Oxford (1967). (Also published as Lawrence Berkeley Laboratory, Report UCRL-17639).

26. D. H. Nelson, "SLFS Calibration" Lawrence Berkeley Laboratory Magnetic Measurements Engineering Book No. 553 (1975).

TECHNICAL INFORMATION DIVISION
LAWRENCE BERKELEY LABORATORY
UNIVERSITY OF CALIFORNIA
BERKELEY, CALIFORNIA 94720